Open

Oncogene (2012) 31, 3597–3606

www.nature.com/onc

ORIGINAL ARTICLE

Cytokinesis failure due to derailed integrin traffic induces aneuploidy and oncogenic transformation *in vitro* and *in vivo*

G Högnäs[1,2,5], S Tuomi[1,2,5], S Veltel[1,2], E Mattila[1,2], A Murumägi[3], H Edgren[3], O Kallioniemi[3] and J Ivaska[1,2,4]

[1]*Medical Biotechnology, VTT Technical Research Centre of Finland, Turku, Finland;* [2]*Turku Centre for Biotechnology, University of Turku, Turku, Finland;* [3]*FIMM, Institute of Molecular Medicine, University of Helsinki, Helsinki, Finland and* [4]*Department of Biochemistry and Food Chemistry, University of Turku, Turku, Finland*

Aneuploidy is frequently detected in solid tumors but the mechanisms regulating the generation of aneuploidy and their relevance in cancer initiation remain under debate and are incompletely characterized. Spatial and temporal regulation of integrin traffic is critical for cell migration and cytokinesis. Impaired integrin endocytosis, because of the loss of Rab21 small GTPase or mutations in the integrin β-subunit cytoplasmic tail, induces failure of cytokinesis *in vitro*. Here, we describe that repeatedly failed cytokinesis, because of impaired traffic, is sufficient to trigger the generation of aneuploid cells, which display characteristics of oncogenic transformation *in vitro* and are tumorigenic *in vivo*. Furthermore, in an *in vivo* mouse xenograft model, non-transformed cells with impaired integrin traffic formed tumors with a long latency. More detailed investigation of these tumors revealed that the tumor cells were aneuploid. Therefore, abnormal integrin traffic was linked with generation of aneuploidy and cell transformation also *in vivo*. In human prostate and ovarian cancer samples, downregulation of Rab21 correlates with increased malignancy. Loss-of-function experiments demonstrate that long-term depletion of Rab21 is sufficient to induce chromosome number aberrations in normal human epithelial cells. These data are the first to demonstrate that impaired integrin traffic is sufficient to induce conversion of non-transformed cells to tumorigenic cells *in vitro* and *in vivo*.
Oncogene (2012) **31,** 3597–3606; doi:10.1038/onc.2011.527; published online 28 November 2011

Keywords: integrin traffic; cytokinesis; aneuploidy; cancer

Introduction

Aneuploidy is thought to be a major contributor of tumor formation. A large fraction of solid tumors are aneuploid and human cells transformed *in vitro* usually develop chromosomal deviations (Hahn *et al*., 1999; Li *et al*., 2000). Recently, evidence has emerged supporting a primary role for aneuploidy in promoting tumorigenesis. Mouse models where loss of mitotic proteins results in impaired cell division and induction of aneuploidy, are prone to tumors with a relatively long latency (Michel *et al*., 2001; Iwanaga *et al*., 2007; Jeganathan *et al*., 2007; Sotillo *et al*., 2007; Weaver *et al*., 2007). Furthermore, aneuploidy has also been shown to increase susceptibility to carcinogen-induced tumor formation (Holland and Cleveland, 2009). Polyploid cells are thought to act as an intermediate state during aneuploidy formation. Tetraploidy or near-tetraploidy has been detected in premalignant conditions and early stage cancers, such as Barrett's esophagus and localized cervical cancer (Galipeau *et al*., 1996; Olaharski *et al*., 2006). Impaired cytokinesis results in multinucleation, chromosomal abnormalities and tumor formation in mice (Fujiwara *et al*., 2005; Rosario *et al*., 2010).

Despite these findings, the role of aneuploidy in tumorigenesis remains unclear, as chromosomal deviations, especially extra chromosome copies, often cause a proliferative disadvantage both on the organism and cellular level (Sotillo *et al*., 2007; Torres *et al*., 2007; Williams *et al*., 2008). It is therefore important to elucidate under which conditions aneuploidy promotes or suppresses tumorigenesis, and which molecular changes actually promote transformation.

Cell adhesion to the matrix is primarily mediated by integrins, which are a family of heterodimeric cell surface receptors composed of an α- and a β-subunit (Giancotti and Ruoslahti, 1999). Normal cells grow in an anchorage-dependent manner and detachment from matrix results in impaired cytokinesis and binucleation (Ben-Ze'ev and Raz, 1981; Kanada *et al*., 2005; Reverte *et al*., 2006; Thullberg *et al*., 2007). Furthermore, loss of β1-integrin expression impairs cytokinesis of chondrocytes *in vivo* (Aszodi *et al*., 2003). Therefore, proper cell attachment to the surrounding matrix is a prerequisite for successful cell division. Integrins are constantly endocytosed from the cell surface and recycled back to the membrane to facilitate formation of new adhesion sites. Integrin traffic is critical for adhesion site disassembly, cell migration, invasion and metastasis (Caswell and Norman, 2008; Ezratty *et al*., 2009; Muller

Correspondence: Professor J Ivaska, Turku Centre for Biotechnology, VTT Technical Research Centre of Finland, University of Turku, Turku 20520, Finland.
E-mail: Johanna.ivaska@vtt.fi
[5]These authors contributed equally to this work.
Received 21 May 2011; revised 10 September 2011; accepted 12 October 2011; published online 28 November 2011

et al., 2009; Ivaska and Heino, 2010). Recruitment of integrin cargo to small GTPase Rab21 is involved in the endocytosis and recycling of β1-integrins en-route to the plasma membrane in migrating cells. In addition, integrin traffic to and from the cleavage furrow is required for completion of cytokinesis and inhibition of Rab21 induces failure in cytokinesis (Pellinen *et al*., 2008). Most matrix-binding integrins share a common β1-subunit paired with any of the 12 different α-subunits. Thus, the β1-subunit is of critical importance in cell adhesion *in vitro* and *in vivo* (Fassler and Meyer, 1995). In many cell types, β1-integrins are internalized via a clathrin-mediated endocytosis route. Previous work has demonstrated that two conserved NPXY motifs of the cytoplasmic domains of β1-integrins are critical for integrin endocytosis (Ng *et al*., 1999; Parsons *et al*., 2002; Pellinen *et al*., 2008). β1YYFF mutant mouse embryonic fibroblasts (MEFs), in which tyrosine residues 783 and 795 in the NPXY-motifs have been substituted with phenylalanines (Czuchra *et al*., 2006) are unable to traffic their integrins and fail cytokinesis when adhering via α/β1-integrin heterodimers (Pellinen *et al*., 2008).

Derailed endocytosis has been linked to cancer and defective vesicular trafficking of integrin adhesion complexes is emerging as a multifaceted hallmark of malignant cells (Mosesson *et al*., 2008) and a critical regulator of cell behavior and signaling (Scita and Di Fiore, 2010). Here, we show that downregulation of Rab21 correlates with increased malignancy in prostate and ovarian cancer samples. We find that derailed integrin traffic, because of loss of Rab21 or expression of mutant β1-integrin, is sufficient to induce aneuploidy in cells. Furthermore, impaired integrin traffic is also sufficient to trigger the generation of chromosomally abnormal aneuploid and tumorigenic cells *in vivo*. Taken together, these data highlight a possible link with defective integrin traffic and the generation of aneuploid tumorigenic cells.

Results

Rab21 is downregulated in human cancer samples

Recently, we described that small GTPase Rab21 regulates integrin targeting during cell division and that spatially and temporally orchestrated endo/exocytic traffic of β1-integrin is critical for execution of normal cytokinesis in adherent cells (Pellinen *et al*., 2008). Generation of tetraploid cells has been suggested as a possible source of chromosomally abnormal aneuploid cells, which are detected in the majority of human solid tumors. Interestingly, we found that Rab21 mRNA expression was significantly downregulated in prostate cancer metastasis compared with samples of normal prostate epithelium (Figure 1a). In addition, expression analysis of published ovarian carcinoma samples demonstrated a very significant downregulation of Rab21 in malignant tissue samples compared with the normal samples (Figure 1b).

The downregulation of Rab21 in these clinical samples could reflect a role for Rab21 in maintaining

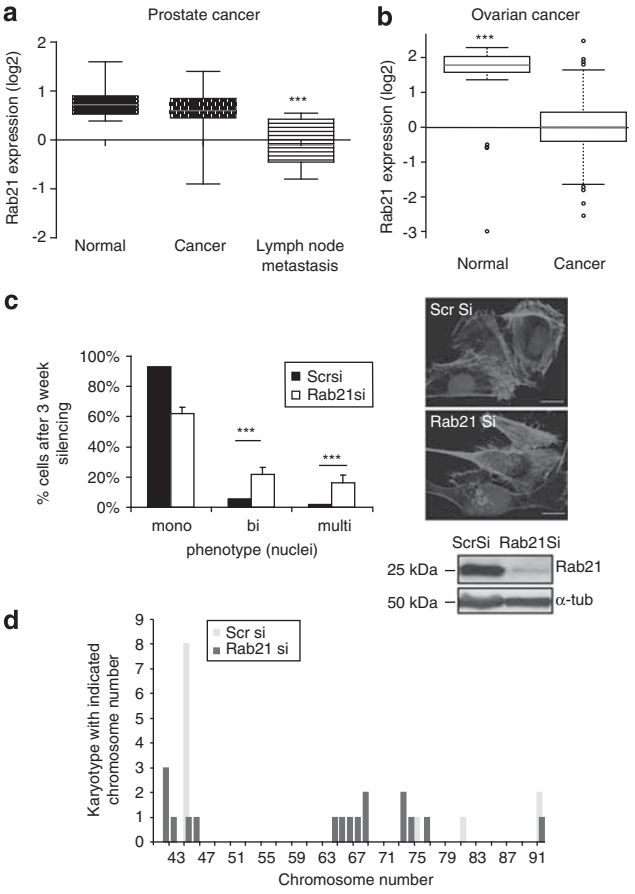

Figure 1 Loss of Rab21 correlates with increased malignancy and is sufficient to induce aneuploidy. (**a**, **b**) Box-plot meta-analysis of *RAB21* mRNA expression in clinical human prostate cancer primary tumors and lymph-node metastasis (**a**) and ovarian carcinoma samples (**b**) compared with the corresponding normal tissues. The colored lines in the box-blots indicate median expression. ($n=111$ samples for prostate and 967 for ovarian, $^{***}P<0.001$). (**c**) Normal human human mammary epithelial cell (HMEC) cells were silenced for 3 weeks with the indicated small interfering RNAs (siRNAs), stained for phalloidin (green) and 4,6-diamidino-2-phenylindole (DAPI) (nuclei, blue) (scale bar 10 μm) and the phenotypes were quantified (mean ± s.e.m., $n=25$–39 cells, $^{***}P<0.005$). (**d**) Chromosome numbers determined from metaphase spreads 2 weeks after the 3-week silencing was discontinued to allow for investigation of sustained and irreversible aneuploidy generated as a result of 3 weeks of continued Rab21 silencing ($n=12$–17 cells per group). A full colour version of this figure is available at the *Oncogene* journal online

a normal cell phenotype. To investigate this, we analyzed the effects of extended silencing of Rab21 in normal human mammary epithelial cells. In line with our previous findings in human cancer cell lines, continuous inhibition of Rab21 for 3 weeks resulted in accumulation of bi- and multinuclear cells (Figure 1c). Furthermore, Rab21 silencing was sufficient to induce aneuploidy. Two weeks after finishing the 3-week silencing, we investigated whether the accumulation of bi- and multinuclear cells had resulted in irreversible aneuploidy, which would be retained even after Rab21 levels return to normal (because of the discontinued RNA interference treatment). The chromosome number

of the control small interfering RNA and Rab21 small interfering RNA-treated cells was analyzed. The majority (8/12 cells) of the Scr small interfering RNA-transfected cells were diploid with 46 chromosomes. In contrast, the chromosome numbers detected from metaphase spreads of Rab21 silenced cells were highly variable with 10/17 cells having a near-triploid chromosome number and 16/17 of the cells being aneuploid (Figure 1d). Thus, loss of Rab21 is sufficient to generate aneuploidy *in vitro* and correlates with malignant disease in human clinical samples.

Derailed integrin traffic in β1-mutant cells results in cytokinesis failure and induction of aneuploidy

In addition to Rab21 inhibition, mutagenesis of β1-integrin cytoplasmic domains (tyrosine residues were mutated to phenylalanines: β1YY783,795FF; here on referred to as β1YYFF) results in impaired integrin traffic and failure of cytokinesis in cells cultured on β1-integrin-specific matrixes (Pellinen *et al*., 2008). As long-term exposure of cells to repeated RNA interference transfection may have adverse effects on cells, we used a mouse model with these mutant integrins to further investigate the consequences of repeated failure of cytokinesis induced by impaired integrin traffic. To this end, two clones each of β1wt and β1YYFF MEFs isolated and cloned from E13.5 embryos, which carry the mutation in germline (Czuchra *et al*., 2006), were used. Immortalization was done with SV40 large T, which in primary MEFs is accompanied by conversion to stable tetraploidy (a total chromosome number of 80) without transforming the cells (Weaver *et al*., 2007). In line with previous work, β1YYFF MEFs were unable to internalize β1-integrins (Supplementary Figure S1a) and execute cytokinesis on β1-specific matrix molecules like collagen and laminin (Figure 2a; Supplementary Movies S1 and S2). Subsequently, these cells became binucleate compared with the normal cytokinesis of the wild-type cells (β1wt_L0).

To investigate the functional outcome of repeated cytokinesis failure, β1wt and β1YYFF cells were plated on the β1-specific matrix component laminin to allow for one cycle of cell division. Subsequently, cells were allowed to grow to confluency in the presence of 10% fetal bovine serum (FBS) (which allows for adhesion via β1 and β3 integrins and thus execution of normal cytokinesis in both cell types). This procedure was repeated four times (L4 for four rounds on laminin) (Figure 2b), after which all of the surviving cells were grown continuously as cell lines for numerous passages under identical conditions on plastic. The karyotypes of the parental β1wt_L0 and β1YYFF_L0 clones a and b were similar with a chromosome number close to tetraploid (4N = 80, Figure 2c, top), as determined by counting chromosomes from metaphase spreads. After four passages on the β1 matrix followed with normal passaging on plastic, both β1YYFF clones showed increased aneuploidy with modal chromosome numbers around 64 (Figure 2c, bottom). Importantly, these altered karyotypes appeared stable as the phenotype of the L4 cells has been retained in the cells passaged on plastic for >2 years. In contrast, identical passaging of the β1wt clones on laminin had no obvious effects on the karyotype. As both independent β1YYFF clones had reached near triploid chromosome number and had similar phenotypes, the β1YYFFa clone was chosen for further studies.

To verify the aneuploidy detected by counting chromosomes, a multi-color fluorescence *in situ* hybridization analysis was carried out from six metaphases from the β1YYFF_L0a and β1YYFF_L4a cells. The majority of the β1YYFF_L0a samples had either a near-diploid or a tetraploid chromosome number. In the β1YYFF_L4a samples on the other hand, only one cell was near-tetraploid and the rest were aneuploid with chromosome numbers ranging from 53 to 83. In all six cells analyzed there were also several structural aberrations in the chromosomes, such as translocations, deletions, fusions, chromosome fragments and dicentric chromosomes. The multi-color fluorescence *in situ* hybridization analysis also showed variations in the copy number of individual chromosomes between β1YYFF_L4a cells. Representative images from the metaphases are shown in Figure 2d.

Array-based comparative genomic hybridization assay was carried out to explore the nature of the chromosomal copy number changes (Supplementary Figure S1b). This assay revealed a small number of defined chromosomal copy number alterations in β1YYFF_L4a. This indicates that the predominant change in β1YYFF_L4a cells compared with β1YYFF_L0a cells are gross chromosomal changes (aneuploidy), not regional deletions and amplifications.

Aneuploid cells display hallmarks of cell transformation in vitro

To investigate how the acquired aneuploidy has affected cell behavior, integrin expression and cell proliferation rates were investigated. No significant difference was detected in total or cell surface β1-integrin expression between β1wt_L0a and L4a or β1YYFF_L0a and L4a cells (Supplementary Figure S2). β1wt_L0a and β1YYFF_L0a cells showed similar growth rates when proliferating on plastic (Supplementary Figure S3a). However, after plating on β1 matrix for four passages, which renders the cells aneuploid, the β1YYFF_L4a cells proliferated significantly more slowly than wild-type cells, which had undergone the same treatment (Supplementary Figure S3b). This is in line with the notion that aneuploidy inhibits proliferation *in vitro* under normal growth conditions (Williams *et al*., 2008).

Two hallmarks of cancer are the ability of cells to grow without anchorage and independently of growth factors (Hanahan and Weinberg, 2000). We observed a significant difference in the capability of anchorage-independent growth between the samples. Only the aneuploid β1YYFF_L4a cells showed a steady increase in proliferation after 24 h (Figure 3a). Furthermore, the aneuploid β1YYFF_L4a cells showed significantly increased growth factor-independent proliferation (Figure 3b) and resistance to cell death induced by tumor necrosis factor-α treatment (Figure 3c) when

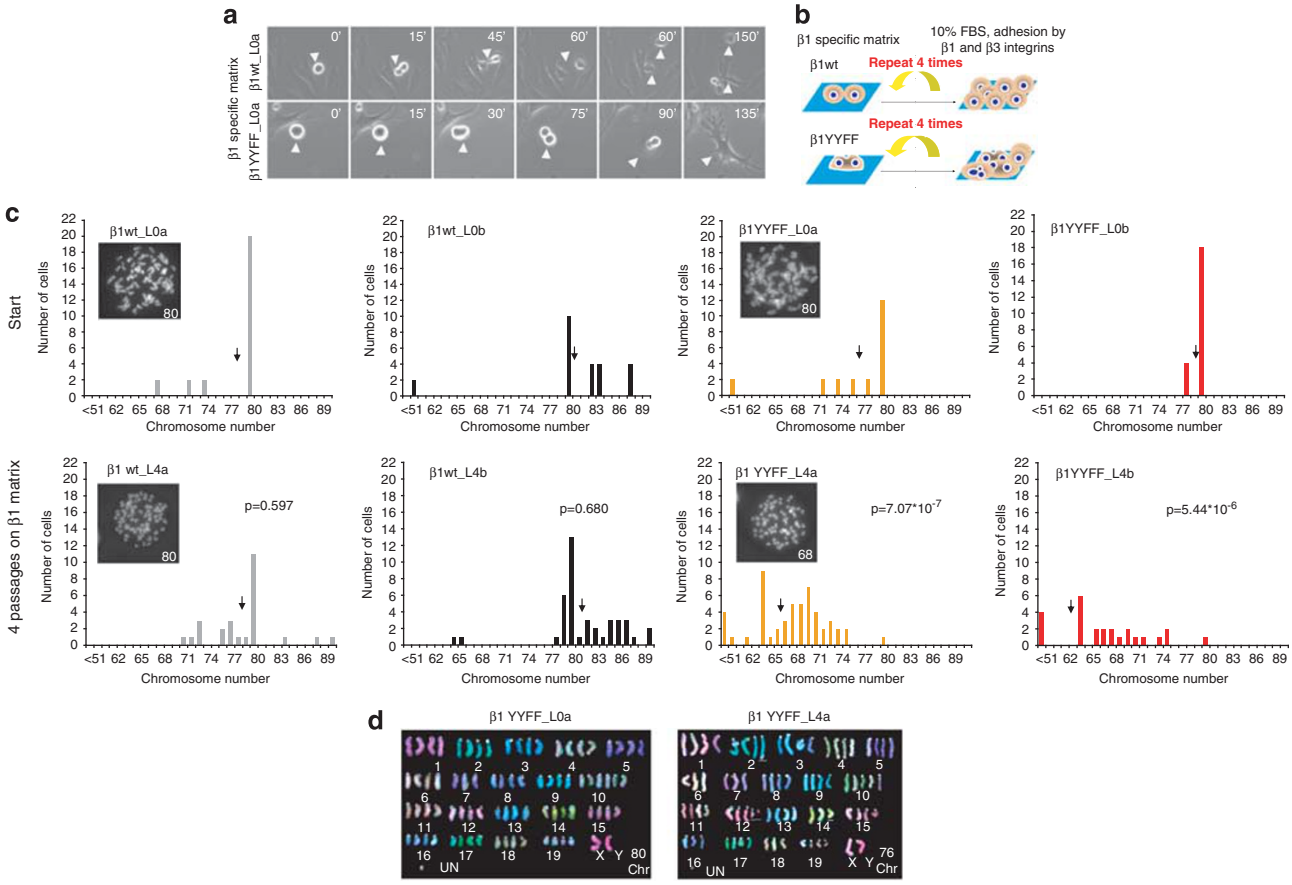

Figure 2 Derailed integrin traffic in β1-cytoplasmic tail mutant MEFs results in cytokinesis failure and induction of aneuploidy. (**a**) β1YYFF cells become binucleate on a β1-specific matrix. Representative still images of time-lapse analysis of β1YYFF_L0a and β1wt_L0a cells undergoing cytokinesis on a β1-integrin-specific matrix. Arrowheads indicate cells undergoing division and the resulting daughter cells. Numbers indicate minutes. (**b**) A schematic image of the experiment. β1wt and β1YYFF cells were plated on the β1-specific matrix component laminin to allow for one cell division. Subsequently, cells were allowed to grow to confluency in the presence of 10% FBS (allowing for β3-integrin-mediated adhesion) and this procedure was repeated four times after which all cell lines were continuously passaged under normal condition on plastic. (**c**) Chromosome numbers determined from metaphase spreads at the beginning and after four passages on β1 matrix ($n = 25$–52 cells per group). Representative chromosome spreads are shown as insets with the number of chromosomes indicated. Arrows indicate mean chromosome number in each population. The *P*-values indicate the statistical difference in chromosome numbers of the cell lines before and after laminin treatment. (**d**) Karyotyping using multi-color fluorescence *in situ* hybridization (mFISH) of β1YYFF_L0a and β1YYFF_L4a shows structural and numerical aberrations in β1YYFF_L4a. 6 metaphases per cell line were analyzed.

compared with the stable tetraploid control cells. Thus, aneuploidy is linked to acquisition of several properties of malignant cells.

Members of the Ras subfamily of small GTPases are often hyperactivated in cancer and thereby influence and deregulate many intracellular signaling pathways. However, introduction of oncogenic Ras to normal cells induces cellular senescence rather than cell transformation, suggesting that other alterations are also required for cell transformation (Serrano *et al*., 1997). Interestingly, we found that introduction of H-RasV12 to the aneuploid β1YYFF_L4a dramatically increased their foci growth and anchorage-independent proliferation in soft agar compared with the same cells transfected with the empty control plasmid (Figure 3d). This suggests that aneuploidy-related changes in these cells have rendered them more susceptible to Ras-induced transformation. In contrast, Ras-transfected β1YYFF_L0a were not able to grow in soft agar or grow as foci (Figure 3d). In fact, RasV12 slightly inhibited foci growth in the parental β1YYFF_L0a cells, thus supporting the perception that these cells are untransformed. Introduction of H-RasV12 to β1wt-L0a and L4a cells did not induce growth of large colonies in soft agar (Figure 3d). Taken together, these data demonstrate that repeated failure of cytokinesis because of impaired integrin traffic is sufficient to cause aneuploidy and induce cell transformation *in vitro*.

Aneuploid β1YYFF_L4 cells are invasive in vitro

We observed that the β1YYFF_L4a cells had gained the ability to execute cytokinesis normally on β1-specific matrix with occasional multipolar mitoses (Figures 4a and b; Supplementary Movies S2 and S3) compared with the impaired cell division of β1YYFF_L0a cells (Supplementary Movie S1). This suggested that

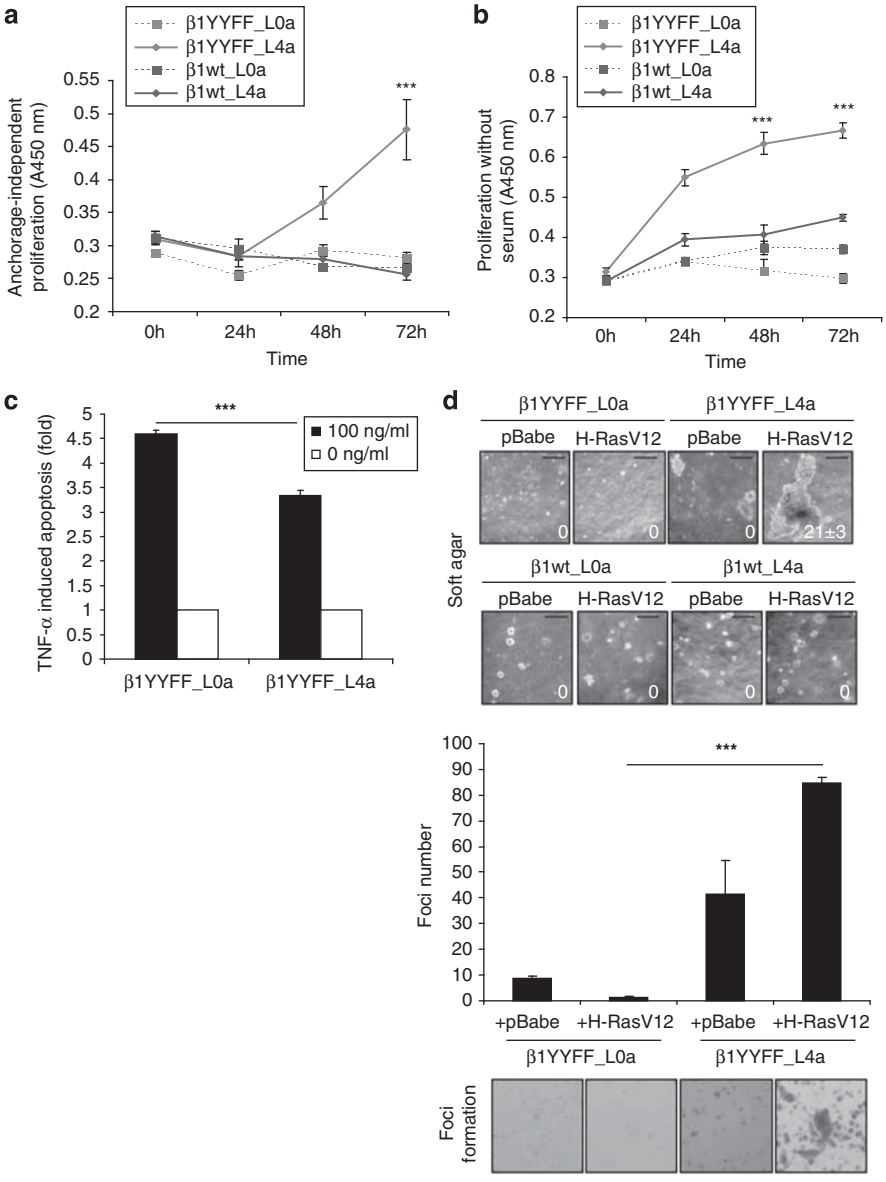

Figure 3 Induction of aneuploidy results in cell transformation *in vitro*. (**a**) Anchorage-independent proliferation of the indicated cell lines on 1% agarose gel for 72 h was analyzed by using WST-1 and measuring absorbance at 450 nm (mean ± s.e.m., $n=4$; ***$P<0.05$). (**b**) Proliferation of the indicated cell lines was analyzed in serum free medium using WST-1 (mean ± s.e.m., $n=4$; ***$P<0.001$). (**c**) Apoptosis was scored using Apo-ONE reagent from the indicated cell lines with or without 24-h tumor necrosis factor-α (TNF-α) treatment (mean ± s.e.m., $n=4$; ***$P<0.001$). (**d**) H-RasV12 or pBabe (control)-transfected cells were grown in soft agar for 23 days or allowed to form foci on plastic during 6 days. Graph shows quantification of foci number and representative images of foci and soft agar colonies from the indicated cells (mean ± s.d, $n=3$; ***$P<0.001$). Numbers in the soft agar panels indicate mean number of very large colonies per well. A full colour version of this figure is available at the *Oncogene* journal online

impaired integrin traffic, causative to the cytokinesis defect of the parental β1YYFF_L0a cells, would be somehow restored or compensated by another mechanism in the aneuploid cells. Indeed, the generated aneuploid β1YYFF_L4a cells had gained the ability to endocytose their β1-integrin compared with the untransformed β1YYFF_L0a cells (Figure 4c). The restored integrin traffic could be partly via a clathrin-independent pathway, as integrin endocytosis in the β1YYFF_L4a cells was less sensitive to clathrin inhibitor monodansylcadaverin (MDC) than endocytosis in the β1wt_L4a cells (β1wt_L4a cells 44 ± 2% and β1YYFF_L4a 24 ± 2% inhibition during 20-min endocytosis by MDC). Thus, induction of aneuploidy had allowed for selection of a cell population with altered integrin traffic allowing the cells to circumvent the disadvantage imposed by the expression of a mutant β1-integrin.

Integrin traffic is closely linked with cell migration and invasion both *in vitro* and *in vivo* and highly invasive cells display increased integrin traffic (Caswell and Norman, 2008). Therefore, we wanted to investigate whether the transformed phenotype is associated with altered invasive properties. The aneuploid β1YYF-

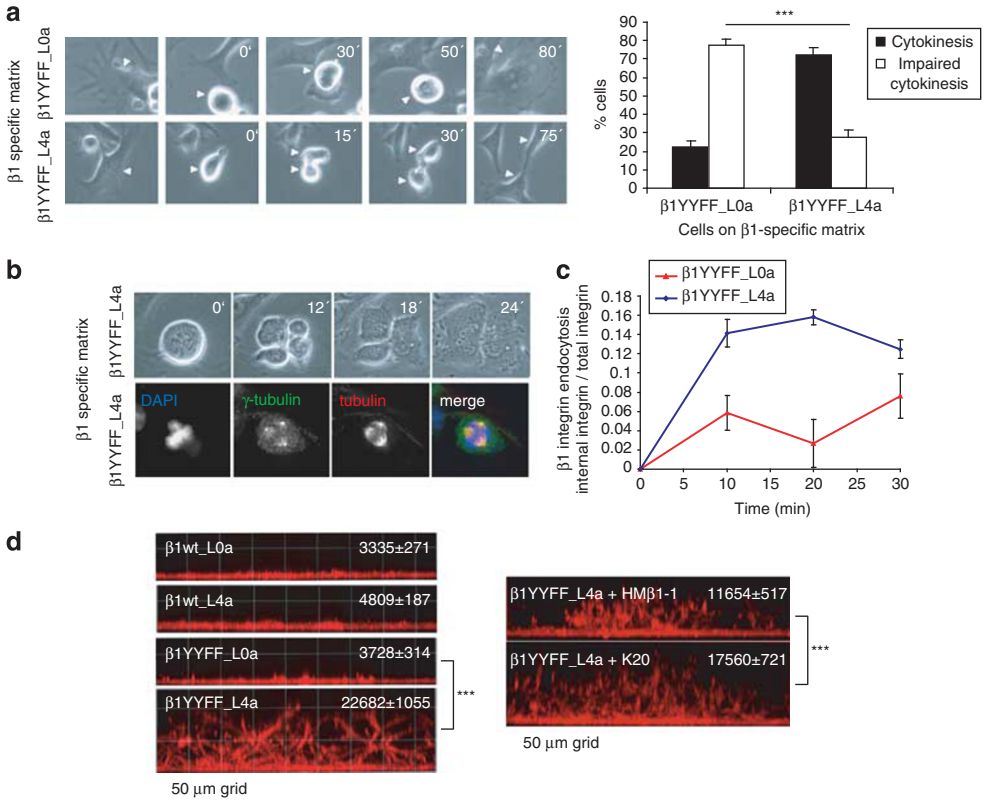

Figure 4 β1YYFF_L4a cells have regained the ability to divide on β1-specific matrixes and traffic integrins. (**a**) Representative still images of time-lapse analysis of β1YYFF_L0a and β1YYFF_L4a cells undergoing cytokinesis on a β1-integrin-specific matrix. Graph shows quantification of cell division phenotypes (mean ± s.e.m., 94–108 cells from three experiments, $***P = <0.0005$). Numbers indicate minutes. (**b**) Representative micrographs and still images of time-lapse analysis of β1YYFF_L4a cells undergoing cytokinesis on a β1-integrin-specific matrix. Numbers indicate minutes. Cells were stained as indicated. (**c**) Biochemical analysis of endocytosis of cell surface biotinylated β1 integrin in β1YYFF_L4a and β1YYFF_L0a cells (mean ± s.e.m., $n = 3$). (**d**) The indicated cells were allowed to invade in growth factor reduced Matrigel for 4 days in the presence or absence of β1-function blocking antibody, after which the cells were fixed and stained with Alexa 546-phalloidin. Representative side view images of the invading cells, 50 μm grid. Numbers indicate the invasion area (pixels). All numerical data are representative from three or more independent experiments (mean ± s.e.m., $n = 4$; $***P < 0.005$).

F_L4a cells were able to invade efficiently into Matrigel, which was applied on top of adhered cells on plastic (Figure 4d). This was integrin dependent because blocking β1-integrin adhesion to the ECM with an anti-β1 antibody significantly reduced β1YYFF_L4a invasion into Matrigel (Figure 4d). None of the tetraploid control cells β1YYFF_L0a, β1wt_L0a and β1wt_L4a showed any invasive capacity and only formed a monolayer of cells underneath the Matrigel plugs.

Derailed integrin traffic results in aneuploidy and tumorigenesis in vivo

To assess the tumorigenic potential of these cells *in vivo*, athymic nude mice were subcutaneously injected with β1YYFF_L0a, β1YYFF_L4a, β1wt_L0a and β1wt_L4a cells and monitored for tumor formation for 7 weeks. Animals injected with wild-type MEFs did not form tumors, while all 10 mice injected with aneuploid β1YYFF_L4a cells rapidly started developing tumors at the injection site, and these tumors grew steadily during 6 weeks to a final average area of $\sim 64\,mm^2$ (Figure 5a). Intriguingly, the 10 mice injected with non-transformed β1YYFF_L0a cells showed very slow tumor development after a nearly 3-week latency reaching a final average tumor area of $\sim 18\,mm^2$, suggesting that these cells have become transformed and tumorigenic during the experiment *in vivo*. Histological analysis of the tumors confirmed them to be highly malignant fibrosarcomas or rhabdomyosarcomas of grade 3/3 or 4/4 (Figure 5b).

Cell lines were generated from the xenografts in order to analyze them in more detail and to determine whether their ploidy had been altered *in vivo*. Metaphase spreads made from four of the established β1YYFF_L4a tumor cell lines demonstrated aneuploidy with chromosome numbers between 52 and 80 (Figure 5c). Aneuploidy was also verified by karyotyping six metaphases from one of the tumor cell lines. The number of chromosomes ranged from 51 to 74 (Figure 5d displays a cell with 68 chromosomes) and 5 out of 6 cells also showed structural aberrations. Out of 393 chromosomes, 41 had structural rearrangements (~10%), but none of these were recurrent. Taken together, these data confirm that generation of aneuploidy in this model was sufficient to induce transformation of cells that were tumorigenic also *in vivo*.

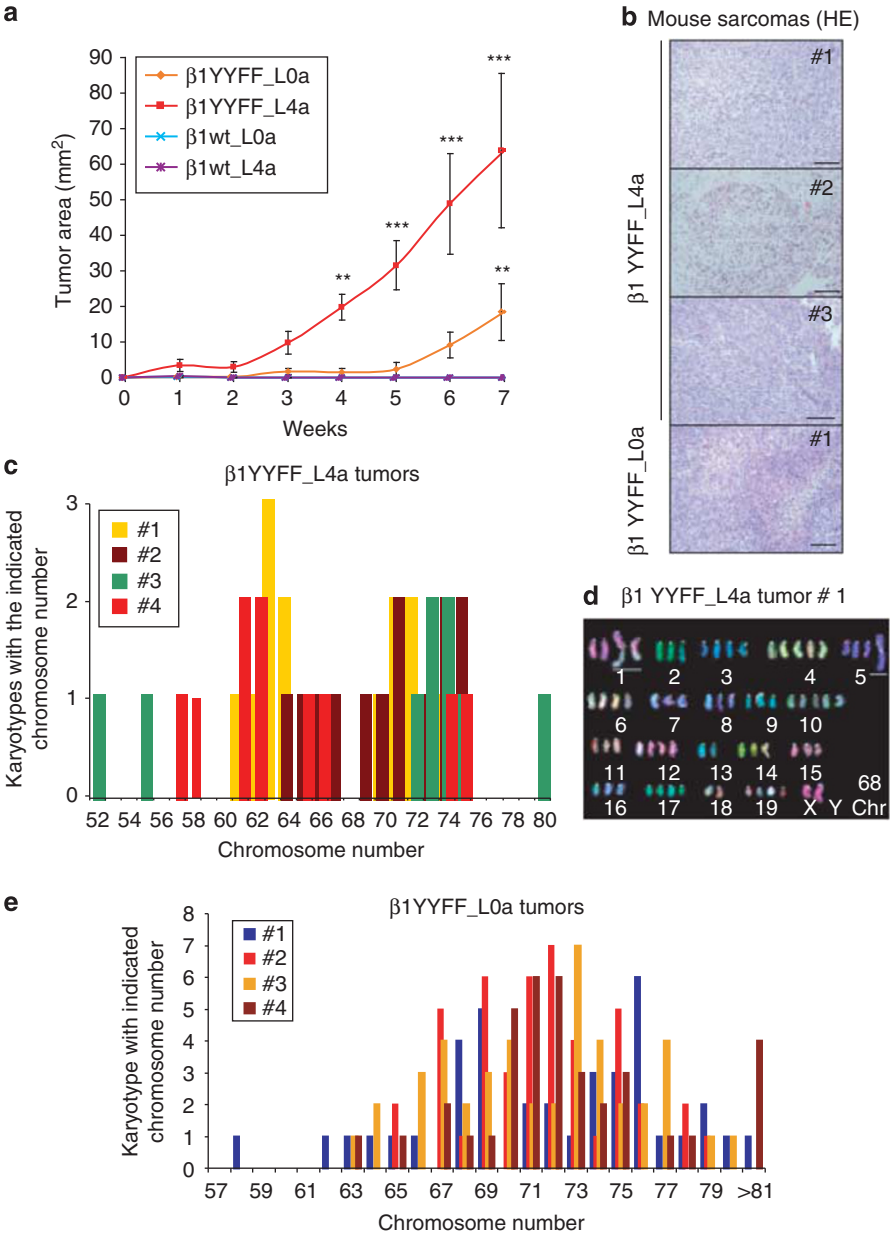

Figure 5 Impaired integrin traffic induces aneuploidy and tumor formation also *in vivo*. (**a**) Mean tumor area (mm²) 0–7 weeks after injection. The tumor progression for each sample group during the whole experiment is shown (the growth curves of the β1wt sample groups are not visible) (mean ± s.e.m., $n=10$; $^{**}P<0.005$, $^{***}P<0.0005$). (**b**) Hematoxylin and eosin (HE) staining of sarcomas from mice injected with β1YYFF_L0a or β1YYFF_L4a cells, scale bar 100 μm. (**c**) Quantification of chromosome numbers of tumor cell lines from β1YYFF_L4a mice ($n=9$–13 cells per group). All cell lines are aneuploid. (**d**) Karyotype of a β1YYFF_L4a-derived tumor cell line shows structural and numerical aberrations. Six metaphases were analyzed. (**e**) Quantification of chromosome numbers of tumor cell lines from β1YYFF_L0a mice ($n=39$–51 cells per group). All cell lines are aneuploid.

However, we were interested to analyze the tumors generated with long latency from the non-transformed, stable tetraploid β1YYFF_L0a cells in mice. We generated four cell lines from individual tumors and analyzed them in more detail. Interestingly, we found that, unlike the parental cells introduced to the mice, these cells were also aneuploid with chromosome numbers ranging from 58 to over 81. Therefore, these data demonstrate that impaired integrin traffic is sufficient to induce aneuploidy and malignant transformation in cells also *in vivo*.

Discussion

Homeostasis of tissues is regulated by cell matrix interactions and changes in the tumor microenvironment are linked with tumor progression and increased malignancy. Cell adhesion is critical for normal cell division and impaired integrin function because of loss of Rab21 or mutations in the integrin cytoplasmic domain results in generation of multinuclear cells *in vitro* (Ben-Ze'ev and Raz, 1981; Reverte *et al*., 2006; Pellinen *et al*., 2008). Multinucleate, polyploid cells are

thought to act as genetically unstable intermediates during cancer formation. Here, we show that loss of Rab21 is linked with cancer progression in human prostate cancer and ovarian carcinoma samples. Furthermore, we demonstrated that derailed integrin traffic resulting in failed cytokinesis can generate aneuploidy. Our results show that (1) these aneuploid cells are transformed and tumorigenic *in vivo*, (2) aneuploidy has induced phenotypic changes in cells, which allow them to compensate for the disadvantage linked to the expression of the mutant β1-integrin and (3) impaired integrin traffic is sufficient to give rise to aneuploidy and cell transformation also *in vivo*. Importantly, no drugs or chemicals were used in this study; instead, a mutation in integrin β1 that prevents normal cell division on specific matrixes was used as a means to induce repeated cytokinesis failure and aneuploidy.

Aneuploidy is as such growth inhibiting, but may actually promote evolution toward improved proliferation in an aneuploid state (Torres *et al*., 2008). Our data imply that induction of massive aneuploidy generates a multitude of cells with altered phenotypes and local requirements dictate that alterations provide mutant cells with a selective advantage. As an example, we find that the β1YYFF_L4a cells have regained the ability to traffic β1-integrin and this most likely contributes also to the increased invasiveness of these cells.

It is becoming increasingly evident that alterations in endocytic traffic are a common feature in cancer cells. Therefore, the fact that altered endocytic traffic of cell adhesion receptors can induce aneuploidy and transformation is fundamentally important and conceptually novel. A tumor-associated β1-integrin mutation has been detected in squamous cell carcinoma (Evans *et al*., 2003), but integrin mutations are otherwise rare in cancer. However, we show here that loss of Rab21 expression can be detected in human cancer samples with increased malignancy. This may turn out to be clinically relevant if the degree of aneuploidy was analyzed alongside Rab21 expression levels in clinical samples. Interestingly, cells that lack the small GTPase Rab21 become bi-and multinucleate in culture because of reduced integrin traffic and failure of cytokinesis (Pellinen *et al*., 2008). Furthermore, we find that extended silencing of Rab21 is sufficient to generate aneuploid cells *in vitro*. Defects in integrin traffic may therefore contribute to genetic instability of human cancers.

Many of the mouse models of repeated failure to segregate one or a few chromosomes per division have led to tumor formation with long latencies (Weaver *et al*., 2007; Holland and Cleveland, 2009). In contrast, generation of aneuploidy via polyploid intermediates induced by cytokinesis failure or overexpression of Mad2 seems to be more severe in terms of selection for favorable chromosomal aberrations and generation of highly malignant cells (Fujiwara *et al*., 2005; Sotillo *et al*., 2007; Rosario *et al*., 2010). This was also the case in our model, where induction of aneuploidy *in vitro* gave rise to highly tumorigenic cells capable of growing very quickly as sarcomas in mice. Importantly, we also found that non-aneuploid cells with impaired integrin traffic gave rise to aneuploid tumors with long latency *in vivo*. This is to the best of our knowledge the first experimental demonstration of the link between impaired integrin traffic and tumorigenesis *in vivo*. In addition, these data demonstrate that generation of aneuploid offspring is sufficient to generate tumorigenic cells without exogenous expression of known oncogenes or inhibition of bona fide tumor-suppressor genes.

Materials and methods

Cell culture

Mouse embryonic fibroblasts from β1wt and β1YYFF mice were prepared from E13.5 embryos of heterozygous matings as previously described (Czuchra *et al*., 2006). Cells were immortalized with the SV40 large T as described by Pellinen *et al*. (2008) and cultured in high glucose Dulbecco's modified Eagle's medium supplemented with 10% FBS, 2 mM L-glutamine and 1% penicillin/streptomycin. Human mammary epithelial cells were cultured in F12 HAM: high glucose Dulbecco's modified Eagle's medium in a 1:1 ratio supplemented with 1% FBS, 2 mM L-glutamine, 10 μg/ml insulin, 0,5 μg/ml hydrocortisone, 20 ng/ml epidermal growth factor and 50 ng/ml choleratoxin. Small interfering RNA-mediated silencing was done using HiPerfect transfection reagent (Qiagen, Valencia, CA, USA) and DNA constructs were transfected with Lipofectamine 2000 (Invitrogen, Carlsbad, CA, USA) according to the manufacturer's protocol.

Chromosome spreads and multi-color fluorescence in situ *hybridization analysis*

Cells were grown to ~80% confluency in a 10 cm plate, 1 μM nocodazole was added to the medium and the cells were incubated ~5 h at 37 °C. The media and trypsin-detached cells were pooled and pelleted by centrifugation, after which the pellet was resuspended in 3–5 ml 75 mM KCl and allowed to stand for 10 min at room temperature. Five drops of fix (3:1 methanol:acetic acid) was added, cells pelleted and the supernatant removed with ~250 μl remaining in which the cells were resuspended. In all, 3–5 ml fix was added dropwise while vortexing gently. Cells were fixed overnight at 4 °C and the pellet was washed twice in 1 ml fix the following day. Cells were resuspended in 100 μl residual fix and dropped onto a methanol-wiped microscope glass. The samples were dried in a fume hood 10 s and on an 80 °C heat plate 30 s. In total, 40 μl Vectashield (Vector Labs, Burlingame, CA, USA) mounting medium containing 4,6-diamidino-2-phenylindole was added for nuclear staining. For the multi-color fluorescence *in situ* hybridization analysis, cells were incubated with 0.2 μg/ml colcemid (Invitrogen) for 3–4 h, trypsinized and pelleted by centrifugation at 1110 r.p.m. 10 min. The supernatant was removed except for 0.5 ml and the pellet resuspended by gently flicking the tube. In all, 10 ml 75 mM KCl was added dropwise while flicking. The cells were incubated at room temperature for 10 min, pelleted and resuspended as above. 2–3 ml fixative (3:1 methanol:acetic acid) was added while flicking, after which the tube was filled up with fixative and incubated at −20 °C for 30 min. Cells were pelleted and resuspended as above, fixative was again added as above. Cells were finally resuspended in 1 ml fixative and analyzed at Chrombios GmbH (Raubling, Germany).

Cell proliferation and apoptosis assays

The wells of a Costar 96-well plate with clear bottom (Corning Inc., Corning, NY, USA) were either left untreated or coated with 1% agarose in phosphate-buffered saline (PBS) (for

anchorage-independent growth) and 5–10 × 10^3 cells in 100 μl medium was added to the wells. To measure proliferation, the cells were incubated with 10 μl WST-1 reagent (Roche Applied Science, Indianapolis, IN, USA) for 1 h at 37 °C. Absorbance was measured at 450 nm on Envision Multilabel plate reader (PerkinElmer, Waltham, MA, USA). For the apoptosis assay, 2.5 × 10^4 cells in 100 μl medium containing 5% FBS were applied to the wells of a 96-well plate. After 24 h, 10 μg/ml cycloheximide (Sigma-Aldrich, St Louis, MO, USA) and 100 ng/ml tumor necrosis factor-α (Peprotech Inc., Rocky Hill, NJ, USA) was added. After another 24 h, the cells were incubated with one sample volume of Apo-ONE Caspase-3/7 reagent (Promega Corporation, Madison, WI, USA) at room temperature for 1 h. Apoptosis was determined by measuring the absorbance at 485 nm.

Transformation assays
For the soft agar assay, a 1 ml layer of a 1:1 mix of 2 × media and 1.2% agar in PBS was plated on the bottom of a 24-well plate well. After solidification of the gel at 4 °C for 10 min, 600 μl of 2.5 × 10^5 cells/ml in a 1:1 mix of 2 × media and 0.6% agar was added on top of the bottom gel. After solidification, the gel was overlaid with 500 μl medium and incubated at 37 °C for 23 days. In the foci formation assay, 750 cells were applied on six-well plate wells in triplicates and allowed to grow for 6 days. The cells were fixed with methanol for 30 min and stained with 0.05% crystal violet 30 min, followed by washing in PBS and drying.

Invasion assays
In all, 25% Growth Factor Reduced Matrigel in Dulbecco's modified Eagle's medium was added on top of ~70% confluent cells on an eight-well μ-Slide (ibidi GmbH) and the gel was allowed to polymerize ~3 h at 37 °C before adding medium containing 2% FBS. Cells were allowed to invade for 4 days, while successively increasing the serum content of the medium to 8%. The cells were fixed with 4% paraformaldehyde for 20 min at 37 °C, washed with buffer (1% bovine serum albumin, 2 mM MgCl2, 5 mM EGTA in PBS) and permeabilized with 0.3% Triton X-100 in wash buffer for 10 min at room temperature. Cells were stained with 1:40 Alexa phalloidin-546 in wash buffer overnight at 4 °C. Invasion was visualized using a Zeiss microscope (Carl Zeiss Microscopy, LLC, Thornwood, NY, USA) with a spinning disk confocal unit and SlideBook 5.0 imaging software (Intelligent Imaging Innovations Inc., Denver, CO, USA). Z intervals of 1.87 μm were taken with a 20 × objective. The images were analyzed with the NIH ImageJ software package (Bethesda, MD, USA). For blocking of β1-integrin, cells were pre-incubated with 10 μg/ml Low Endotoxin, Azide-Free (LEAF) purified anti-mouse/rat CD29 clone HMβ1-1 (Biolegend, San Diego, CA, USA) or control CD29 antibody K20 (Beckman Coulter Immunotech, Marseille, France) before invasion into Matrigel supplemented with 10 μg/ml antibody.

In vivo *experiments*
All animal experiments were performed in accordance with relevant national regulations and were approved by an animal license (ESLM-2008-08600/Ym-23). In all, 1 × 10^6 cells suspended in 200 μl PBS were subcutaneously injected into the left flank of 8 weeks old female athymic nude mice, with 10 mice each per cell group. Samples from the biggest tumors were fixed in formalin 24 h at room temperature, followed by washing under cold, running tap water for 1 h and immersion in 70% EtOH. The samples were embedded in paraffin and slices taken for hematoxylin and eosin staining. The sections were analyzed by Dr Jukka Laine at the Department of Pathology, Turku University Hospital.

Array-CGH
β1YYFF_L4a MEFs were analyzed on the 244K Mouse Genome CGH oligonucleotide microarray (G4415A) following the direct method of the November 2008, version 6 protocol (Agilent Technologies, Santa Clara, CA, USA). Genomic DNA was extracted using DNeasy Blood and Tissue kit (Qiagen) according to the manufacturer's instructions. β1YYFF_L0a sample was used as reference sample. In total, 3 μg of digested sample or reference DNA was labeled with Cy5-dUTP and Cy3-dUTP, respectively, according to the protocol. Labeled samples were pooled and hybridized onto an array. These data were processed by a laser confocal scanner and Feature Extraction software (Agilent) according to the manufacturer's instructions. The copy number changes were analyzed with DNA Analytics software, version 4 (Agilent).

Time-lapse analysis
In live cell imaging of MEF cells, phase-contrast images were taken with a Zeiss inverted wide-field microscope (EL Plan-Neofluar 20 × /0.5 NA objective, 4–6 frames/h) equipped with a heated chamber (37° C) and CO_2 controller (4.8%). Cells were imaged with 1–15 min frame interval for total of 3–12 h. Image analysis and video construction was done with imaging software NIH ImageJ. Statistical analyses were performed using Student's *t*-test.

Conflict of interest

The authors declare no conflict of interest.

Acknowledgements

We thank Dr M Karin for DNA constructs; H Marttila, J Siivonen and L Lahtinen for excellent technical assistance. I Ahonen is thanked for help with the statistical analysis. This research has been supported by ERC starting grant, Academy of Finland, Finnish Cancer Organizations and Sigrid Juselius Foundation. GH is supported by Turku Graduate School for Biomedical Sciences, ST by VTT Medical Biotechnology and SV is supported by EMBO LTF and Alexander von Humboldt foundation. The Central Animal Laboratory of the University of Turku is acknowledged for the animal experiments.

References

Aszodi A, Hunziker EB, Brakebusch C, Fassler R. (2003). Beta1 integrins regulate chondrocyte rotation, G1 progression, and cytokinesis. *Genes Dev* **17**: 2465–2479.

Ben-Ze'ev A, Raz A. (1981). Multinucleation and inhibition of cytokinesis in suspended cells: Reversal upon reattachment to a substrate. *Cell* **26**: 107–115.

Caswell P, Norman J. (2008). Endocytic transport of integrins during cell migration and invasion. *Trends Cell Biol* **18**: 257–263.
Czuchra A, Meyer H, Legate KR, Brakebusch C, Fassler R. (2006). Genetic analysis of beta1 integrin 'activation motifs' in mice. *J Cell Biol* **174**: 889–899.
Evans RD, Perkins VC, Henry A, Stephens PE, Robinson MK, Watt FM. (2003). A tumor-associated beta 1 integrin mutation that abrogates epithelial differentiation control. *J Cell Biol* **160**: 589–596.
Ezratty EJ, Bertaux C, Marcantonio EE, Gundersen GG. (2009). Clathrin mediates integrin endocytosis for focal adhesion disassembly in migrating cells. *J Cell Biol* **187**: 733–747.
Fassler R, Meyer M. (1995). Consequences of lack of beta 1 integrin gene expression in mice. *Genes Dev* **9**: 1896–1908.
Fujiwara T, Bandi M, Nitta M, Ivanova EV, Bronson RT, Pellman D. (2005). Cytokinesis failure generating tetraploids promotes tumorigenesis in p53-null cells. *Nature* **437**: 1043–1047.
Galipeau PC, Cowan DS, Sanchez CA, Barrett MT, Emond MJ, Levine DS *et al*. (1996). 17p (p53) allelic losses, 4N (G2/tetraploid) populations, and progression to aneuploidy in barrett's esophagus. *Proc Natl Acad Sci USA* **93**: 7081–7084.
Giancotti FG, Ruoslahti E. (1999). Integrin signaling. *Science* **285**: 1028–1032.
Hahn WC, Counter CM, Lundberg AS, Beijersbergen RL, Brooks MW, Weinberg RA. (1999). Creation of human tumour cells with defined genetic elements. *Nature* **400**: 464–468.
Hanahan D, Weinberg RA. (2000). The hallmarks of cancer. *Cell* **100**: 57–70.
Holland AJ, Cleveland DW. (2009). Boveri revisited: chromosomal instability, aneuploidy and tumorigenesis. *Nat Rev Mol Cell Biol* **10**: 478–487.
Ivaska J, Heino J. (2010). Interplay between cell adhesion and growth factor receptors: from the plasma membrane to the endosomes. *Cell Tissue Res* **339**: 111–120.
Iwanaga Y, Chi YH, Miyazato A, Sheleg S, Haller K, Peloponese JM *et al*. (2007). Heterozygous deletion of mitotic arrest-deficient protein 1 (MAD1) increases the incidence of tumors in mice. *Cancer Res* **67**: 160–166.
Jeganathan K, Malureanu L, Baker DJ, Abraham SC, van Deursen JM. (2007). Bub1 mediates cell death in response to chromosome missegregation and acts to suppress spontaneous tumorigenesis. *J Cell Biol* **179**: 255–267.
Kanada M, Nagasaki A, Uyeda TQ. (2005). Adhesion-dependent and contractile ring-independent equatorial furrowing during cytokinesis in mammalian cells. *Mol Biol Cell* **16**: 3865–3872.
Li R, Sonik A, Stindl R, Rasnick D, Duesberg P. (2000). Aneuploidy vs gene mutation hypothesis of cancer: recent study claims mutation but is found to support aneuploidy. *Proc Natl Acad Sci USA* **97**: 3236–3241.
Michel LS, Liberal V, Chatterjee A, Kirchwegger R, Pasche B, Gerald W *et al*. (2001). MAD2 haplo-insufficiency causes premature anaphase and chromosome instability in mammalian cells. *Nature* **409**: 355–359.
Mosesson Y, Mills GB, Yarden Y. (2008). Derailed endocytosis: an emerging feature of cancer. *Nat Rev Cancer* **8**: 835–850.
Muller PA, Caswell PT, Doyle B, Iwanicki MP, Tan EH, Karim S *et al*. (2009). Mutant p53 drives invasion by promoting integrin recycling. *Cell* **139**: 1327–1341.
Ng T, Shima D, Squire A, Bastiaens PI, Gschmeissner S, Humphries MJ *et al*. (1999). PKCalpha regulates beta1 integrin-dependent cell motility through association and control of integrin traffic. *EMBO J* **18**: 3909–3923.
Olaharski AJ, Sotelo R, Solorza-Luna G, Gonsebatt ME, Guzman P, Mohar A *et al*. (2006). Tetraploidy and chromosomal instability are early events during cervical carcinogenesis. *Carcinogenesis* **27**: 337–343.
Parsons M, Keppler MD, Kline A, Messent A, Humphries MJ, Gilchrist R *et al*. (2002). Site-directed perturbation of protein kinase C- integrin interaction blocks carcinoma cell chemotaxis. *Mol Cell Biol* **22**: 5897–5911.
Pellinen T, Tuomi S, Arjonen A, Wolf M, Edgren H, Meyer H *et al*. (2008). Integrin trafficking regulated by Rab21 is necessary for cytokinesis. *Dev Cell* **15**: 371–385.
Reverte CG, Benware A, Jones CW, LaFlamme SE. (2006). Perturbing integrin function inhibits microtubule growth from centrosomes, spindle assembly, and cytokinesis. *J Cell Biol* **174**: 491–497.
Rosario CO, Ko MA, Haffani YZ, Gladdy RA, Paderova J, Pollett A *et al*. (2010). Plk4 is required for cytokinesis and maintenance of chromosomal stability. *Proc Natl Acad Sci USA* **107**: 6888–6893.
Scita G, Di Fiore PP. (2010). The endocytic matrix. *Nature* **463**: 464–473.
Serrano M, Lin AW, McCurrach ME, Beach D, Lowe SW. (1997). Oncogenic ras provokes premature cell senescence associated with accumulation of p53 and p16INK4a. *Cell* **88**: 593–602.
Sotillo R, Hernando E, Diaz-Rodriguez E, Teruya-Feldstein J, Cordon-Cardo C, Lowe SW *et al*. (2007). Mad2 overexpression promotes aneuploidy and tumorigenesis in mice. *Cancer Cell* **11**: 9–23.
Thullberg M, Gad A, Le Guyader S, Stromblad S. (2007). Oncogenic H-ras V12 promotes anchorage-independent cytokinesis in human fibroblasts. *Proc Natl Acad Sci USA* **104**: 20338–20343.
Torres EM, Sokolsky T, Tucker CM, Chan LY, Boselli M, Dunham MJ *et al*. (2007). Effects of aneuploidy on cellular physiology and cell division in haploid yeast. *Science* **317**: 916–924.
Torres EM, Williams BR, Amon A. (2008). Aneuploidy: cells losing their balance. *Genetics* **179**: 737–746.
Weaver BA, Silk AD, Montagna C, Verdier-Pinard P, Cleveland DW. (2007). Aneuploidy acts both oncogenically and as a tumor suppressor. *Cancer Cell* **11**: 25–36.
Williams BR, Prabhu VR, Hunter KE, Glazier CM, Whittaker CA, Housman DE *et al*. (2008). Aneuploidy affects proliferation and spontaneous immortalization in mammalian cells. *Science* **322**: 703–709.

Supplementary Information accompanies the paper on the Oncogene website (http://www.nature.com/onc)